Nonlinear analysis of sloshing in rigid rectangular tank under harmonic excitation

Kishore Chandra Biswal †, Santosh Kumar Nayak *

† Department of Civil Engineering, National Institute of Technology Rourkela, Odisha, India
* Department of Civil Engineering, National Institute of Technology Rourkela, Odisha, India
Presenting authors email: kcb@yahoo.co.in

Abstract

The present study delves into the effect of nonlinearity on the dynamic behavior of liquid filled rectangular tanks. A velocity potential based 2D Galerkin FEM model has been developed for the simulation. Mixed Eulerian-Lagrangian-material –node time-marching scheme is used for numerical solution at every time step. Fourth-order Runge-Kutta scheme is used for the time-stepping integration of free surface boundary conditions in a Lagrangian manner in order to track the free surface. It is observed that although nonlinearity has no significant effect in the pressure distribution on the tank wall. However nonlinearity has significant bearing on base shear, base moment and sloshing amplitude.

1. Introduction

A substantial chunk of the components of important life line structures and industrial installations comprise of rectangular liquid storage tanks. Such tanks are in extensive use for storage of water, oil, liquefied natural gas, and a variety of other liquids such as chemical fluids and liquid wastes of industries. Since long time, it is amply evident that the dynamic behaviour of partially-filled liquid tank is significantly different from that of a tank of similar geometry and dimension containing solid material. This is due to the complex phenomenon of sloshing. During seismic mishap, damage to such tanks not only amounts to immediate loss of the contained liquid, which results in huge economic loss, but also has far reaching consequences in terms of environmental hazard and human health.

Ever since the pioneer work of Housner [1], a lot of research has been carried out to understand the seismic behaviour of partially-filled liquid containers, yet the multidimensional complexities associated with liquid-tank system unfolded renewed challenges for the researchers. Housner [1] resolved the hydrodynamic response into impulsive and convective components approximated by lumped added-masses and proposed an idealized two-degree of freedom system, with concentrating masses of liquid at two points, to represent their respective modes of vibration. Haroun and Housner [2] developed a linear three-mass model of ground-supported anchored tanks by incorporating wall flexibility into the model and found that impulsive mode of pressure was considerably influenced by wall flexibility. Haroun [3] studied the hydrodynamic response of rigid rectangular tanks considering linear wave theory. Veletsos [4] used Flüggle's shell theory to analyze anchored circular tanks and found that for tanks with realistic flexibility, the impulsive forces are considerably higher than those in rigid walls. The dynamic responses of cylindrical steel tanks in various conditions were investigated by Niwa and Clough [5], Hamdan [6], Hernández-Barrios [7], Bayraktar et al. [8], Estekanchi and Alembagheri [9] and Chen et al. [10]. Hamdan [6] examined the accuracy of design guidelines various codes for the seismic response of cylindrical steel liquid storage tanks and commented on the inadequacy of provisions of design guide lines against many of the commonly occurred failure modes reported during past earthquakes. Kim et al. [11] presented a 3D analytical solution based on Rayleigh-Ritz method and found that impulsive pressure of rectangular tank can be greatly amplified due to wall flexibility. Chen et al. [12] proposed a 2D finite difference model to simulate non-linear seismic finite-amplitude liquid sloshing in rectangular tank. Choun and Yun [13] presented a novel 2D linear analytical solution and studied the seismic response of rectangular tank with a submerged structure. Virella et al. [14] used finite element package ABAQUS and made an observation that nonlinearity of surface wave does not have any major effect on the pressure distribution on the walls of rectangular tanks. Kianoush and Ghaemmaghami [15] developed linear finite element model and studied the effects of earthquake frequency content on the seismic behaviour of concrete rectangular tanks. They used shallow and tall tank configurations on various types of soils and concluded that the frequency contents of earthquakes significantly influence the dynamic behavior of fluid-tank-soil system.

Most of the investigations are focused on the seismic response of cylindrical storage tanks and rectangular tank has received very little attention. Further in many of the studies linear sloshing has been considered for simulation. Hence, numerical simulation of nonlinear sloshing in rigid rectangular tank is considered in the present study. This study assimilates the results on the effect of nonlinear free surface boundary conditions, *vis-a-vis* linear model, on the free vibration characteristics of liquid and the dynamic response parameters of tank. Harmonic motions of forcing frequency equal to the fundamental sloshing frequency are prescribed as external excitations. Also studied is the effect of nonlinearity when the forcing frequency is not very close to the sloshing frequency. Rectangular tanks with different fill-depths (ratio of liquid height to tank width, (*d/L*) are considered in the study.

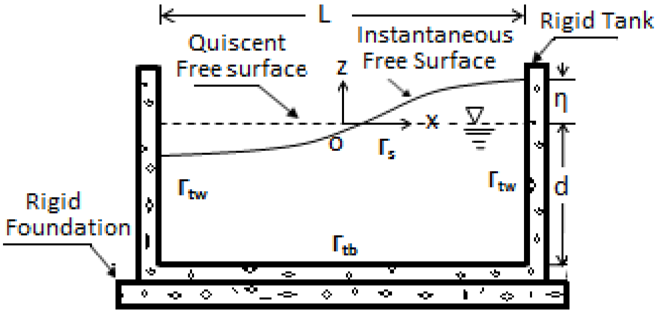

Figure 1. Schematic diagram of tank-liquid system

2. Mathematical modeling of tank-liquid system

Fig.1 shows the problem geometry for the tank-liquid system. The Cartesian coordinate system O-xz for the computational domain of the liquid is defined such that the origin is at the center of the still free surface with z-axis pointing vertically upward. The liquid is assumed to be inviscid and incompressible and the flow is irrotational. For such an ideal liquid, the velocity distribution can be derived by a scalar function called *velocity potential* $\varphi(x, y, t)$ which describes the motion of liquid inside the liquid domain through satisfaction of Laplace (continuity) equation

$$\nabla^2 \varphi = 0 \qquad (1)$$

which governs the potential flow in the fluid domain Ω. Eq. (1) is elliptic in nature and requires both free surface and body surface boundary conditions for simulation of nonlinear sloshing wave problem. The boundary conditions are described are follows.

2.1 Nonlinear free surface boundary conditions

On the time dependent free surface boundary Γ_s, both kinematic and dynamic boundary conditions need to be satisfied at any instant and on the exact free surface. The kinematic boundary condition requires that the fluid particle once on the free surface remains always on the free surface. Based on Eulerian description the free surface kinematic boundary condition is given by

$$\frac{\partial \eta}{\partial t} = \frac{\partial \varphi}{\partial z} - \frac{\partial \varphi}{\partial x}\frac{\partial \eta}{\partial x} \quad \text{on} \quad \Gamma_s \qquad (2)$$

where $\eta(x, z, t)$ is the instantaneous free surface wave elevation.

The dynamic boundary condition requires that the pressure on the free surface be uniform and equal to the external atmospheric pressure. This boundary condition can be obtained from Bernoulli equation with the assumption of zero atmospheric pressure. The effect of viscosity is artificially incorporated into the dynamic free surface boundary condition in simplified manner [16]. The damping modified unsteady Bernoulli's equation may be expressed as

$$\frac{\partial \varphi}{\partial t} = \text{-g}\eta \text{ - } \frac{1}{2}\nabla\varphi.\nabla\varphi\text{- }\mu\varphi \quad \text{on } \Gamma_s \tag{3}$$

where g is the gravitational acceleration.

2.2 Body surface boundary condition

On the walls of the tank the velocity of liquid is equal to the wall velocity in normal direction

$$\frac{\partial \varphi}{\partial n} = V_n \qquad \text{on } \Gamma_w \tag{4}$$

where V_n is the instantaneous velocity of the vertical wall subjected to horizontal ground acceleration and n is the normal to the wall surface pointing out of the liquid domain.

On the rigid bottom supported on rigid foundation, no flux condition needs to satisfied for impermeable body surface

$$\frac{\partial \varphi}{\partial n} = 0 \qquad \text{on } \Gamma_b \tag{5}$$

Thus Eqs. (1) - (5) defines the initial and boundary value problem with nonlinear free surface boundary conditions. The nonlinearity in free surface boundary condition is attributed to: (1) *a priori* unknown free surface elevation at any given instant and (2) kinematic and dynamic boundary conditions in equation (2) and (3) as they contain second order differential terms.

The set of equations (1)-(5) are elliptic in space and parabolic in time. Mixed-Eulerian-Lagrangian method due to Longuet-Higgins and Cokelet [17] is used for numerical solution of the system of equations. In mixed-Lagrangian-Eulerian the surface nodes called 'markers' are allowed to move with the same velocity as the liquid. In this procedure the spatial equations are solved in Eulerian (fixed grid) frame and the integration of the free surface boundary conditions is executed in Lagrangian manner. This requires the free surface boundary conditions in Eq. (2) and (3) to be written in Lagrangian form as follows.

$$\frac{\mathrm{d}\varphi}{\mathrm{d}t} = \text{-g}\eta + \frac{1}{2}\nabla\varphi.\nabla\varphi\text{- }\mu\varphi \quad \text{on } \Gamma_s \tag{6}$$

$$\frac{\mathrm{d}x}{\mathrm{d}t} = \frac{\partial \varphi}{\partial x}\ ; \qquad \frac{\mathrm{d}z}{\mathrm{d}t} = \frac{\partial \varphi}{\partial z} \tag{7}$$

After obtaining the time derivative of velocity potential, the nonlinear hydrodynamic pressure can be calculated by using the following equation:

$$p = -\rho\left(\frac{\partial \varphi}{\partial t} + \frac{1}{2}\left|\nabla\varphi\right|^2 + \mu\varphi\right) \tag{8}$$

The base shear S_b and overturning base moment M_b can be calculated by the following expression

$$S_b = \int_{\Gamma_w} p\,\mathrm{d}\Gamma_w \tag{9}$$

$$M_b = \int_{\Gamma_w} (p\,\mathrm{d}z)z + \int_{\Gamma_b} (p\,\mathrm{d}x)x \tag{10}$$

Impulsive pressure may be determined by assuming the whole liquid as a rigid solid block without convective mass. This assumption ignores the sloshing of the liquid and hence the convective response. As a consequence of this, the pressure at the quiescent liquid free surface vanishes at every instant during the motion.

$$\frac{\partial \varphi}{\partial t}(x,0,t) = 0 \tag{11}$$

3. Finite element formulation

The entire liquid domain Ω, bounded by body surface Γ_w tank bottom Γ_b and free surface Γ_s, is discretized by four-noded quadrilateral elements for finite element formulation and solution of Laplace equation to solve for Dirichlet boundary condition (φ) on the free surface and Neumann boundary condition $(\nabla\varphi)$ on the body surface. The velocity potential may be approximated as

$$\varphi \approx \bar{\varphi}(x,z,t) = \sum_{j=1}^{n} \varphi_j N_j(x,z) \tag{12}$$

where φ_j are time dependent nodal velocity potentials, N_j are shape functions and *n* is the number of nodes. Application of Galerkin's weighted-residual method to Laplace equation gives rise to

$$\int_{\Omega} \nabla^2 \varphi\, N_i \,\mathrm{d}\Omega = 0 \tag{13}$$

Equation (13) may be written as
$$\int_{\Omega} \left[\nabla(\nabla\varphi N_i) - \nabla\varphi \nabla N_i\right] \mathrm{d}\Omega = 0 \tag{14}$$

Application of Gauss theorem produces
$$\int_{\Gamma} N_i \frac{\partial \varphi}{\partial n} \mathrm{d}\Gamma - \int_{\Omega} \nabla\varphi \nabla N_i \,\mathrm{d}\Omega \tag{15}$$

where $\Gamma = \Gamma_w \cup \Gamma_b \cup \Gamma_s$, is the boundary of the liquid domain Ω. Substitution of the approximation function for the potential and the boundary conditions into the above equation yields

$$\int_{\Omega} \nabla N_i \sum_{i=1}^{n} \varphi_j \nabla N_j \,\mathrm{d}\Omega\Big|_{j\notin\Gamma_s} = \int_{\Gamma_W} N_i V_n d\Gamma - \int_{\Omega} \nabla N_i \sum_{i=1}^{n} \varphi_j \nabla N_j \,\mathrm{d}\Omega\Big|_{j\in s} \tag{16}$$

where Γ_s and Γ_b are the free surface and body (vertical wall) surface respectively on which the potential and its normal derivatives are prescribed. The potential on the free surface is known from the free surface boundary condition and the terms corresponding to the surface nodes have therefore been taken to the right hand side. This scheme suggested by Wu and Eatock Taylor [18] was found to be effective in dealing with the singularity at the intersection point between the body surface and free surface on account of the confluence of boundary conditions.

Eq. (16) may be expressed in matrix form as

$$[K]\{\varphi\} = [F] \tag{17}$$

where
$$K_{ij} = \int \nabla N_i \nabla N_j \,\mathrm{d}\Omega \tag{18}$$

$$F_i = \int_{\Gamma_w} N_i V_n d\mathrm{T} - \int_{\Omega} \nabla N_i \sum_{i=1}^{n} \varphi_j \,\nabla N_j \,\mathrm{d}\Omega\Big|_{j\in\Gamma_s} \tag{19}$$

where K_{ij} is the global fluid matrix and F_i is the global right hand side vector. It must be mentioned that the matrix K_{ij} in Eq. (19) varies with time for fully nonlinear problem.

Numerical evaluation of the dynamic and kinematic boundary conditions, Eqs. (6)-(7) require an approximation of velocity at the free surface. Although, direct differentiation of potential approximation via shape functions is a convenient option to obtain the velocity, shape functions however do not guarantee the continuity of its derivatives at the boundary of the elements and may result in lower order, discontinuous velocity with compromised accuracy. The velocity continuity can be ensured by use of higher order FE for potential approximation. In the present study, however C^0 isoparametric rectangular element is used. In order to avoid excessive accumulation of error in the time stepping procedure, the following method is used for velocity recovery.

The two dimensional velocity vector, $U = u_i + v_j$ may be approximated in terms of the same shape functions as used for velocity potential.

$$U = \sum_{j=1}^{n} U_j \, N_j(x, z) \tag{20}$$

Galerkin weighted-residual method is used to approximate the relationship $\nabla\varphi = U$, in the form

$$\int_{\Omega} N_i (\nabla\varphi - U) \, \mathrm{d}\Omega = 0 \tag{21}$$

Substitution of Eqs. (12) and (20) into Eq. (21) yields

$$\int_{\Omega} N_i \frac{\partial N_j}{\partial n} \varphi_j \, \mathrm{d}\Omega = \int_{\Omega} N_i N_j U_j \, \mathrm{d}\Omega \tag{22}$$

In matrix form the above equation can be expressed as

$$[C]\{u\} = [D_1]\{\varphi\} \tag{23}$$

$$[C]\{v\} = [D_2]\{\varphi\} \tag{24}$$

where,

$$[C] = \int_{\Omega} N_i N_j \, \mathrm{d}\Omega \tag{25}$$

$$[D_1] = \int_{\Omega} N_i \frac{\partial N_j}{\partial x} N_j \, \mathrm{d}\Omega \tag{26}$$

$$[D_2] = \int_{\Omega} N_i \frac{\partial N_j}{\partial y} N_j \, \mathrm{d}\Omega \tag{27}$$

and u_i and v_i are the components of velocity vector U_j at node *j*.

From the velocities thus obtained, the updated position of the free surface at the start of the next time step can be found using Eq. (7). The updated value of the velocity potential on the free surface can also be determined from Eq. (6). A new finite element mesh is then generated corresponding to the updated geometry which requires further solution of Laplace equation in the spatial domain, recovery of velocity and time-integration of kinematic and dynamic boundary conditions to advance the solution in time domain.

4. Model Validation

The model validation is established by comparing the present FEM result with Virella et al. [14]. The tank of width 30.675 m and liquid depth 10.73 m with d/L ratio 0.35 is considered for the simulation. A harmonic force of $a_t = 0.01\mathrm{g}\sin\bar{\omega}t$ is applied as base excitation, where $\bar{\omega}$ is taken as the fundamental sloshing frequency ω_1 of the liquid. The liquid considered for the study is water. Figure 1. shows the time variation of free surface displacement at the right hand wall of the tank. The present FEM result compares extremely well with the result of Virella et al. [14].

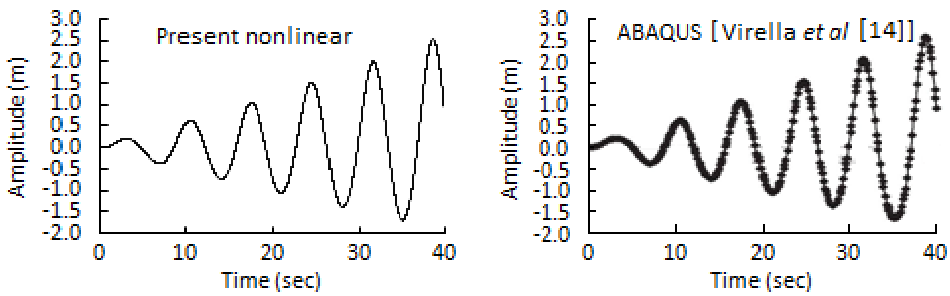

Figure 2. Time history of the sloshing elevation at right hand wall of tank in the first sloshing mode

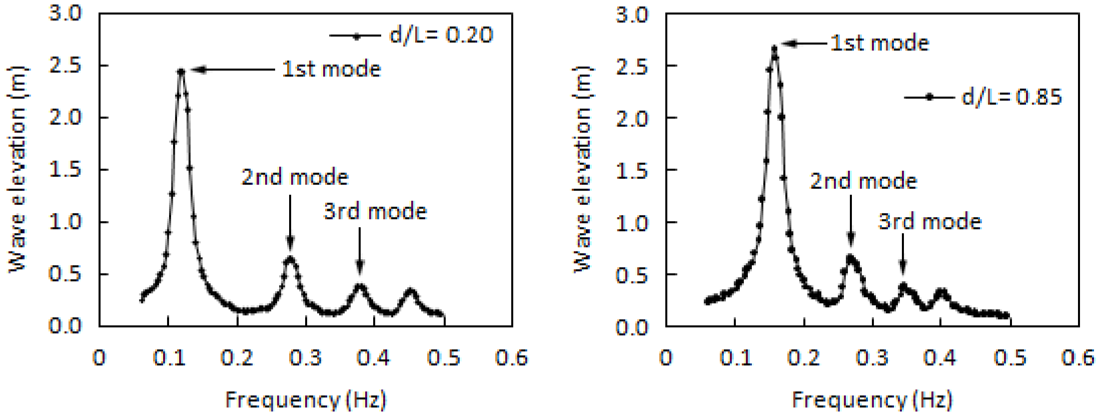

Figure 3. Maximum wave elevation vs. excitation frequency for tank-liquid systems of varying liquid-depths: (a) ***d/ L***= 0.20; (b) ***d/L***= 0.85

5. Numerical Results and Discussions

Rectangular tank of 30 m width and various fill-depths is considered to study the effect of nonlinearity on the dynamic behaviour of the tank-liquid system. Harmonic excitation with same amplitude as in the previous section is used for the study.

5.1 Sloshing Frequencies

The linear frequencies were obtained directly by solving the eigen-value problem from linear finite element model [19]. The nonlinear sloshing frequencies, however, were extracted in an indirect method from harmonic response analysis in the frequency domain. The maximum sloshing elevations, as a function of base excitation frequency, were computed for each of the tank-liquid system with varying depths of liquid. The total time of computation was taken as 40s, which produced more than four cycles of motion in the first natural frequency for any of the selected tank-liquid systems. Figure 3 presents the maximum wave elevation, as a function of base excitation frequency, for systems with various d/L. It is observed that for all the cases the maximum surface wave elevations obtained for their respective first modes are significantly more than those obtained for the higher modes. The sloshing response is dominated by the first sloshing mode. The natural frequencies of first three anti-symmetric sloshing modes are recorded and presented in Table 1. Presented along are their respective linear sloshing modes for comparison. The fundamental frequency increases with increase in the ratio of liquid-depth to tank-width both in case of linear and nonlinear wave theories. The second and third sloshing frequencies, computed from linear theory, remain almost unchanged with increase in the ratio of fill-depth. For the nonlinear second mode, the sloshing frequency showed a marginal decreasing trend. In case of nonlinear third mode the highest reduction in sloshing frequency was observed. The results of natural frequencies for the first three antisymmetric sloshing modes, with linear and nonlinear wave theory, are presented in Figure 4 for easy comparison. Similar variations of natural frequencies were observed both for linear and nonlinear wave theory. Very little variations in natural frequencies are observed between linear and nonlinear theories. The fundamental frequency showed a maximum variation of less than 4.2% for broad tank of *d/L* = 0.2 and less than 3.2% for tall tank of *d/L* = 0.85. The higher mode frequencies are still less affected. Hence, one may conclude that nonlinearity has no significant effect on the natural frequencies.

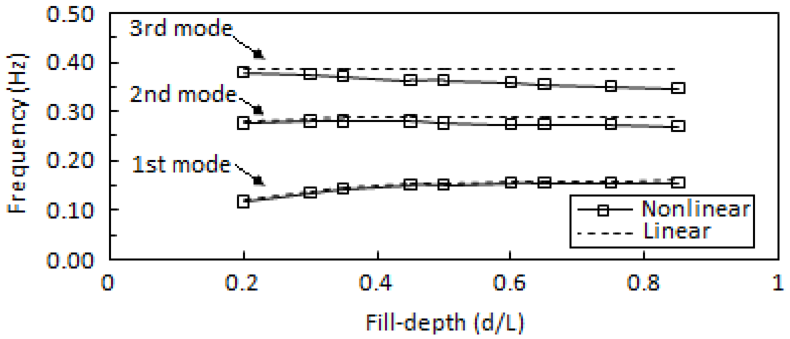

Figure 4. Nonlinear and linear sloshing frequencies for tanks with varying fill depth (***d/L***)

Sl. No.	Fill-depth *(d/L)*	Sloshing modes					
		Linear			Nonlinear		
		First	Second	Third	First	Second	Third
1	0.20	0.121	0.282	0.387	0.116	0.276	0.380
2	0.30	0.139	0.286	0.387	0.136	0.280	0.376
3	0.35	0.145	0.287	0.388	0.144	0.280	0.372
4	0.45	0.152	0.287	0.388	0.152	0.280	0.364
5	0.50	0.155	0.287	0.388	0.152	0.276	0.364
6	0.60	0.158	0.287	0.388	0.156	0.272	0.360
7	0.65	0.159	0.287	0.388	0.156	0.272	0.356
8	0.75	0.160	0.287	0.388	0.156	0.272	0.352
9	0.85	0.161	0.287	0.388	0.156	0.268	0.348

Table 1. Linear and nonlinear natural frequencies for the first three sloshing modes

5.2 Hydrodynamic Pressure Distribution

As stated in the previous section sloshing response is mostly dominated by first mode. Hence, the effect of nonlinearity on the pressure distribution is studied only for the first sloshing mode. Figure 6 shows the comparative result of linear and nonlinear hydrodynamic pressure distributions on the left wall of the tank for two different maximum wave heights of 0.91 m and 1.34 m at the left wall of the tank (d/L = 0.2) having surface profiles as shown in Figure 5. It is observed that the linear analysis yields hydrodynamic force in the conservative side. The difference between the pressure distributions decreased for a large wave height. The height of the resultant force in case of nonlinear pressure distribution is found to be higher. Similar computations are made for rest of the tank-liquid systems, with various fill-depths, considered in the study. In all cases, the linear model yielded conservative result. However, for tanks with fill-depth 0.3 – 0.85, as the wave height increases, an increase in difference of linear and nonlinear pressure distribution is observed. One such observation is presented in Figure 8 for fill-depth of 0.85 with two different sloshing wave heights with deformed surface profile shown in Figure 7.

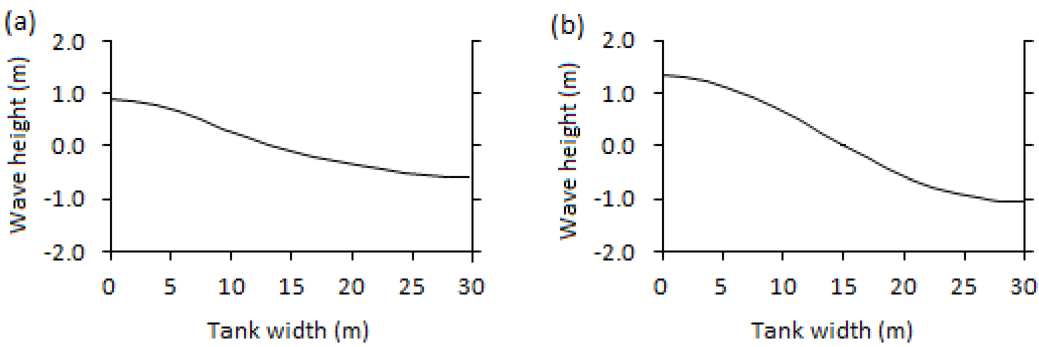

Figure 5. Nonlinear free surface profile for tank-liquid system with fill-depth, ***d/L = 0.2*** corresponding to maximum sloshing wave height at left wall: (a) 0.91 m, (b) 1.34 m

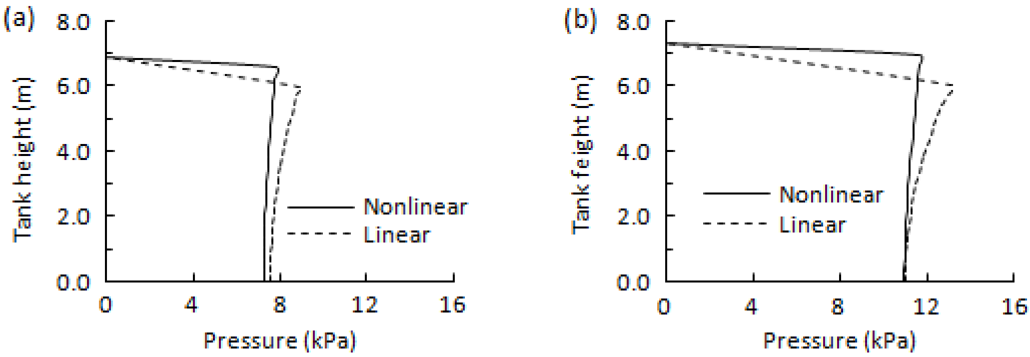

Figure 6. Pressure distribution for first sloshing mode of a tank-liquid system with fill-depth, ***d/L*** = 0.2: (a) wave elevation = 0.91 m, (b) wave elevation = 1.34 m

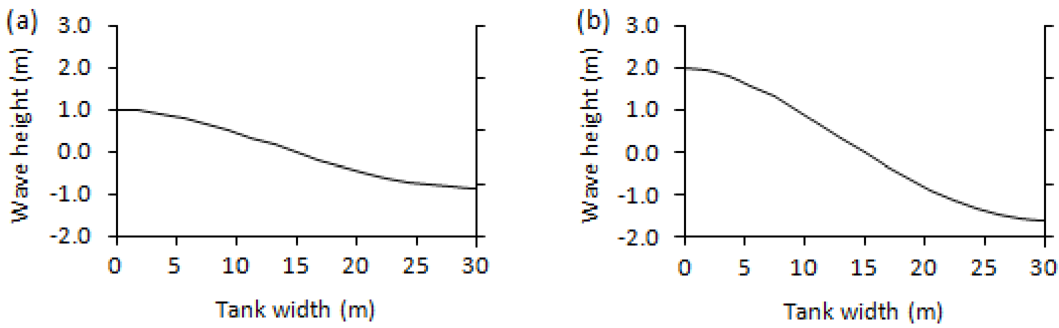

Figure 7. Nonlinear free surface profile for tank-liquid system with fill-depth, ***d/L*** = 0.85 corresponding to maximum sloshing wave height at left wall: (a) 1.0 m, (b) 2.01 m

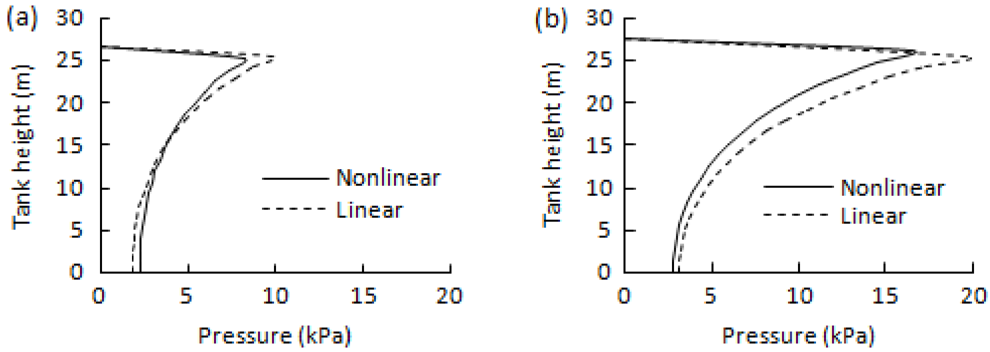

Figure 8. Pressure distribution for first sloshing mode of a tank-liquid system with fill-depth, ***d/L*** = 0.85: (a) wave elevation = 1.0 m, (b) wave elevation = 2.01 m

5.3 Base Shear and over turning base moment

An accurate prediction of the base shear and overturning base moment is essential to ensure the safety of tanks against shell buckling and uplift. To this end, Figure 9-10 present comparative time histories of linear and nonlinear base shear and overturning base moment. One can observe that nonlinear peaks of both base shear and base moments in each cycle are comparatively more than their respective linear counterparts. The linear and nonlinear base shear values, at the corresponding instants at which equal maximum sloshing heights for the respective models occurred, were noted from their respective time histories. It was observed that, for a given value of maximum wave height at the left wall, the linear model gave conservative result which was in consistency with the result in Figure 6 and 8. Similar observation was also made for base moment. Although, nonlinearity of surface wave manifests in terms of significant amplification of wave elevation, it does have major effect on hydrodynamic pressure distribution on the wall, base shear and overturning base moment for a given maximum sloshing elevation at tank wall.

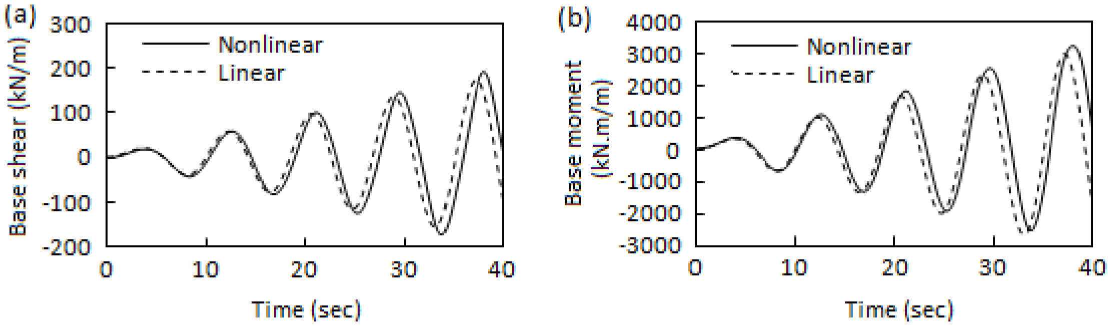

Figure 9. Time history of: (a) base shear and (b) overturning base moment of tank-liquid system with ***d/L*** = 0.2 for first sloshing mode

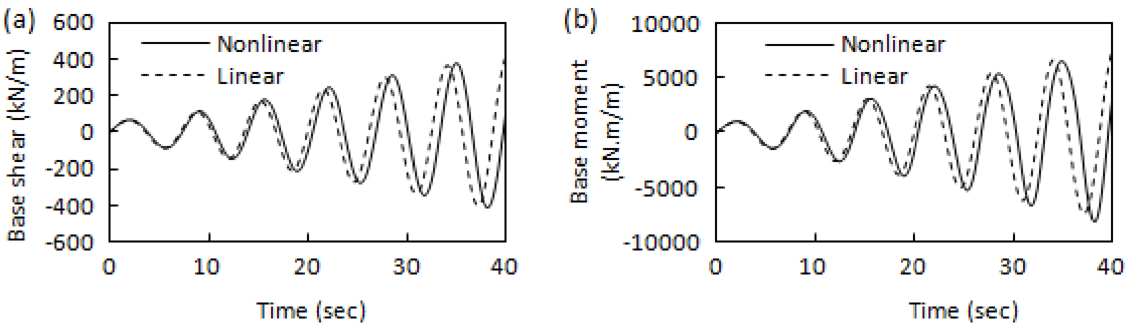

Figure 10. Time history of: (a) base shear and (b) overturning base moment of tank-liquid system with ***d/L*** = 0.85 for first sloshing mode

6. Conclusion

A 2D velocity potential based nonlinear Galerkin finite element model is developed. The model is coded and the simulation is executed in MATLAB platform to investigate the effect of nonlinearity on the dynamic responses of tank-liquid systems with different fill-depths.

Based on the numerical investigation, the following conclusions are drawn.

1. The effect of nonlinearity on the natural sloshing frequencies of the liquid is insignificant irrespective of the fill-depths of the liquid in the tank. And nonlinearity has absolutely insignificant effect on the higher sloshing modes.
2. Nonlinearity has a major effect on the surface wave elevation and should be considered for such decisions as the free board of the tank.
3. Nonlinearity does not have any major effect on the hydrodynamic pressure distribution on the tank wall. However, due to applied hydrodynamic pressures at higher levels of surrounding walls overturning base moment may at times be amplified.
4. Nonlinearity has a considerable effect on the global maximum base shear. The recursion effect of nonlinearity on local peaks should be considered in tank design.
5. The underlined observation is that effect of nonlinearity on dynamic response should not be seen in isolation with respect any predefined sloshing wave height.

7. References

[1] Housner GW, 1963, The dynamic behavior of water tanks, Bull Seismol Soc Amer., 53(2), 381-387.
[2] Haroun MA, Housner GW, 1981, Seismic design of liquid storage tanks. Journal of Technical Councils, ASCE, 107910, 191-207.
[3] Haroun MA, 1984, Stress analysis of rectangular walls under seismically induced hydrodynamic loads, Bull Seismol Soc Amer., 74(3), 1031-1041.

[4] Veletsos AS, 1984, Seismic response and design of liquid storage tanks. Guidelines for the seismic design of oil and gas pipeline systems, ASCE Tech. council on lifeline earthquake engineering, New York, pp. 443-461.
[5] Niwa A, Clough RW, 1982, Buckling of cylindrical liquid-storage tanks under earthquake loading, Earthq Engngr and Struct Dyna, 10, 107–22.
[6] Hamdan FH, 2000, Seismic behaviour of cylindrical steel liquid storage tanks, J. Constr. Steel Res., 53, 307–333.
[7] Hern´andez H, Heredia, E, Alvaro, A, 2007, Nonlinear sloshing response of cylindrical tanks subjected to earthquake ground motion, Eng. Struct., 29, 3364–3376.
[8] Bayraktar A, Sevim B, Can Altunl lk A, Türker T, 2010, Effect of the model updating on the earthquake behaviour of steel storage tanks, J.Constr. Steel Res., 66(3), 462-469.
[9] Estekanchi HE, Alembagheri M, 2012, Seismic analysis of steel liquid storage tanks by Endurance Time method, Thin Wall. Struct., 50(1), 14-23.
[10] Chen YH, Hwang WS, Ko CH, 2007, Sloshing behaviours of rectangular and cylindrical liquid tanks subjected to harmonic and seismic excitations, Earthquake Engng. Struct. Dyn., 36, 1701–1717.
[11] Kim JK, Koh HM, Kwahk IJ, 1996, Dynamic response of rectangular flexible fluid containers, J. Eng Mech., 122(9), 807-17.
[12] Chen W, Haroun MA, Liu F, 1996, Large amplitude liquid sloshing in seismically excited tanks, Earthq Engng Struct. Dyn., 25, 653-669.
[13] Choun Y-S, Yun C-B, 1999, Sloshing analysis of rectangular tanks with a submerged structure by using small-amplitude water wave theory, Earthq Engngr and Struct Dyna, 28, 763-783.
[14] Virella JC, Prato CA, Godoy LA, 2008, Linear and nonlinear 2D finite element analysis of sloshing modes and pressure in rectangular tanks subjected to horizontal harmonic motions, J. Sound Vib., 312(3), 442–60.
[15] Kianoush MR, Ghaemmaghami AR, 2011, The effect of earthquake frequency content on the seismic behaviour concrete rectangular liquid tanks using finite element method incorporating soil- structure interaction, Eng. Struct., 33, 2186-2200.
[16] Faltinsen OM, 1978, A numerical nonlinear method of sloshing in tanks with two-dimensional flow, J. Ship Research, 22(3), 193-202.
[17] Longuet-Higgins MS, Cokelet ED, 1976, The deformation of steep surface wave on water: a numerical method of computation, Proceedings of Royal Society of London, 350, 1-26
[18] Wu GX, Taylor RE, 1994, Finite element analysis of two-dimensional non-linear transient water waves, Applied Ocean Research, 16, 363-372.
[19] Biswal KC, Bhattacharya SK., Sinha PK, 2003, Free-vibration analysis of liquid-filled tank with baffles, J. Sound vib., 259(1), 177-192.